Colloids and Surfaces A 583 (2019) 123992

Contents lists available at ScienceDirect

Colloids and Surfaces A

journal homepage: www.elsevier.com/locate/colsurfa

Unexpected effects of incident radiant energy on evaporation of Water condensate

Tao Ye*, Magdalena Kowacz, Gerald H. Pollack

Department of Bioengineering, University of Washington, Box 355061, Seattle, WA, 98195, United States

GRAPHICAL ABSTRACT

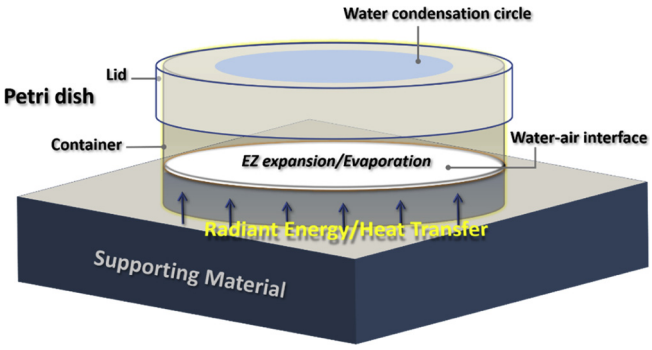

ARTICLE INFO

Keywords:
Water evaporation
Radiant energy
Water/air interfaces
EZ water

ABSTRACT

While water evaporation and condensation are of fundamental importance to our environment, many features remain under investigation. In this study, we explored the water-condensation circle (WCC) formed on the inner surface of Petri dish lids covering containers of water. We found that they progressively diminished in diameter. Surprisingly, the diminution rate could be affected by objects placed beneath the bottom of the container. For systems that were not in thermal equilibrium with the environment (*i.e.*, warm water in the Petri-dish container), thermal conductivity of the materials played the dominant role. Heat transfer from the water in the container to the material beneath affected the temperature of the water and thus the water evaporation, which changed the humidity in the Petri dish and hence the WCC diminution rate. Yet, when no temperature differences existed between the system and the environment, radiant energy emitted by the materials placed beneath the container was a determining factor. This is unexpected. Common materials placed outside chambers of water are not expected to impact evaporation rates.

1. Introduction

Water evaporation and condensation are ubiquitous in nature. They are of vital importance in fields such as the physics of rain, snow, dew, clouds, and fog [1,2], as well as seawater evaporation and distillation [3], internal combustion engines [4], thermal management [5], *etc*. Yet, evaporation and condensation are not well understood. The ocean's surface receives solar radiation, which provides energy for seawater to evaporate to form water vapor. As one of the most important greenhouse gases, water vapor plays a significant role in climate change and global warming [6,7]. Therefore, while water evaporation and condensation have been heavily studied, and models and theories have

* Corresponding author.
E-mail address: yetao@uw.edu (T. Ye).

https://doi.org/10.1016/j.colsurfa.2019.123992
Received 29 July 2019; Received in revised form 6 September 2019; Accepted 16 September 2019
Available online 17 September 2019
0927-7757/

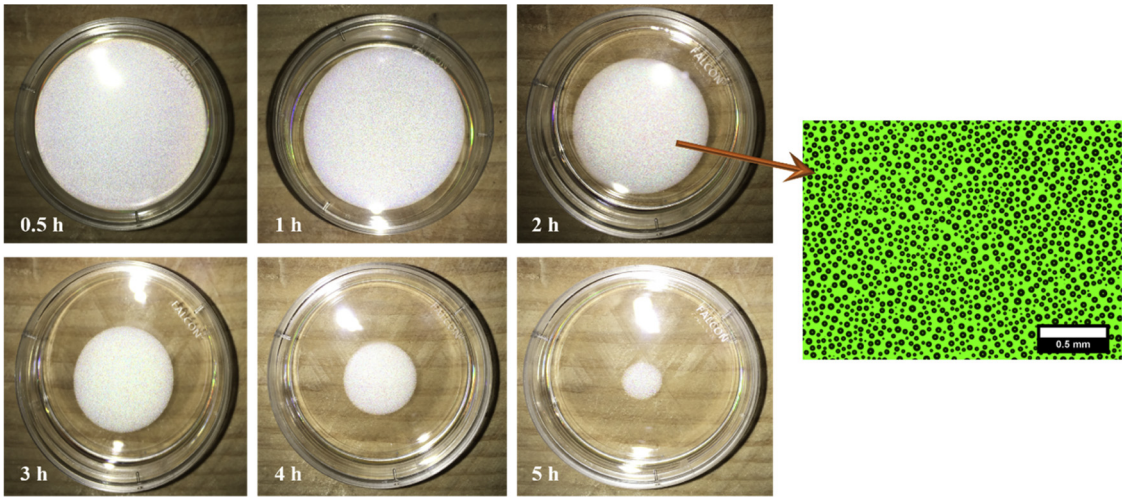

Fig. 1. Progressive diminution of the water-condensation circle (white area) formed on the inner (bottom) surface of the Petri-dish lid. This circle of water condensation is a monolayer of small water droplets lodged next to one another. The right panel is a microscopic image of the small droplets in the water-condensation circle. The black spheres are the water droplets. The average diameter of these droplets was approximately 40 μm. Experimental conditions: 3 mL of 30 °C water in Petri-dish container (35 × 10 mm) covered with the Petri-dish lid. The supporting object beneath the Petri-dish container was wood. Same procedures were conducted for other supporting materials.

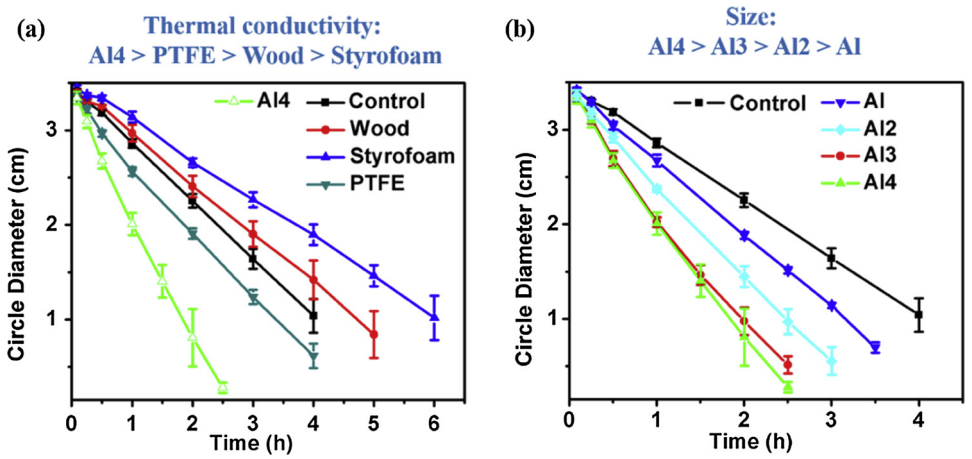

Fig. 2. (a) Effect of different materials placed beneath the Petri-dish containers on the diminution of circle diameter. (b) Effect of aluminum dimensions on the diminution of circle diameter. Experimental condition: 3 mL of 30 °C water in Petri-dish containers (35 × 10 mm, Falcon®).

been developed [8], our knowledge about these phase transitions is limited. Numerous features of water remain to be discovered.

Radiant energy from the sun significantly impacts water evaporation and condensation. These phenomena have been intensively investigated. However, the impacts of radiant energy emitted from common materials on water evaporation and condensation have rarely been explored. A recently discovered type of interfacial water, called "exclusion zone" (EZ) water, may be relevant. EZ water forms at the interface of hydrophilic materials and water as well as at the water-air interface. It builds by utilizing surrounding radiant energy, including incident light and infrared energy [9–12]. Water evaporation and condensation involve the water-air interface. Hence, radiant energy generated by various common materials may influence evaporation and condensation through EZ formation at the water-air interface.

While investigating the impact of radiant energy from different objects on the sedimentation of colloidal particles in water [12], we encountered an unanticipated phenomenon: the progressive diminution of the water-condensation circle (WCC) formed on the inner surface of Petri-dish lids (Fig. 1). This WCC is a monolayer of small water droplets concentrated next to one another to form a circle. We found that the diminution could be affected by objects placed beneath the Petri-dish containers. For systems that were not in thermal equilibrium with the environment (*i.e.*, warm water in the Petri-dish container), the diminution of the WCC, from the periphery inward, could be significantly facilitated by placing highly thermally conductive metals (*e.g.*, brass, aluminum, and stainless steel) beneath, compared to other low thermally conductive objects (*e.g.*, Teflon [PTFE], wood, and Styrofoam). If there were no temperature differences between the system and the environment (*i.e.*, room-temperature water in the Petri-dish container), an unexpected trend was observed: Styrofoam noticeably facilitated the diminution of the WCC, while aluminum significantly prolonged the WCC. Thus, this study was conducted to explore the WCC phenomenon and provide a possible understanding of the underlying mechanisms.

2. Experimental Section

For all the experiments, deionized water (18.2 MΩ cm) was collected from a Barnstead D3750 Nanopure Diamond purification system. Petri dishes (35 x 10 mm, Falcon®, and 95 x 15 mm, Fisherbrand®) were purchased from Fisher Scientific and used without any treatment. Each Petri dish consists of a container and a lid.

Materials used in this study were similar to those used in our previous study [12], and listed as follows: Wood (17 × 9.0 × 1.5,cm, length × width × height), Wood1 (1.0 × 1.0 × 0.8,cm), Wood2

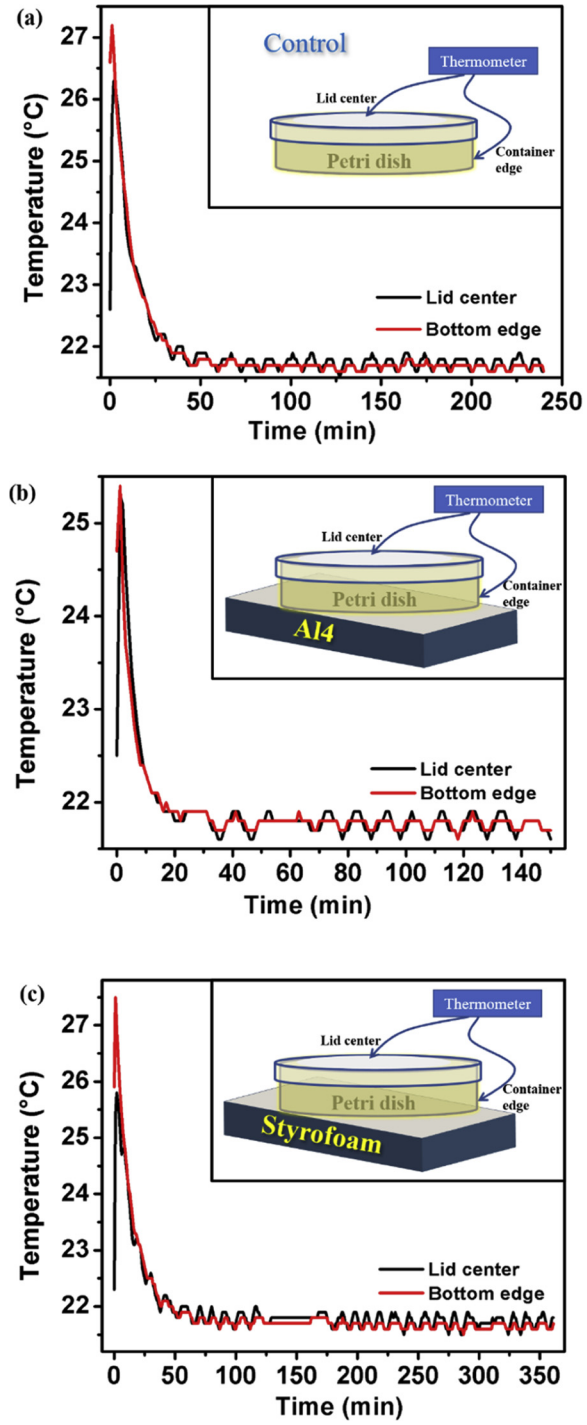

Fig. 3. Temperature changes during the experiments. (a) control, (b) aluminum (Al4), (c) Styrofoam. The arrowheads in the inset schematics indicate the positions where the thermocouple probes were attached. "Lid center" shows the temperature of the lid's outer surface, while the "container edge" shows the temperature of the container's outer surface edge. The temperature was measured using an OMEGAETTE datalogger thermometer HH306A with compact transition ground-junction probes (TJC36 series).

(2 × 2 × 1, cm), Wood3 (2.5 × 2.5 × 1.5,cm); Styrofoam (20.5 × 13.9 × 3.1,cm), Styrofoam1 (4.0 × 2.0 × 4.6,cm), Styrofoam2 (5.5 × 4.5 × 4.6,cm), Styrofoam3 (9.0 × 5.5 × 4.6,cm), Styrofoam4 (10.8 × 9.0 × 4.6,cm); PTFE (18.5 × 9.0 × 2.8,cm), PTFE1 (1.0 × 1.0 × 0.8,cm), PTFE2 (2 × 2 × 1,cm), PTFE3 (2.5 × 2.5 × 1.5,cm); Al (Aluminum, 1 cm cube), Al2 (Aluminum, 2 × 2 × 1,cm), Al3 (Aluminum, 7.3 × 4.6 × 0.8,cm), Al4 (Aluminum, 8 × 4.5 × 2,cm), Al5 (Aluminum disk, diameter: 16.6 cm, height: 1 cm); brass (1.0 × 1.0 × 0.8,cm); and, stainless steel (cylinder, diameter:1.2 cm, height: 0.6 cm). The numbers following the material type (*e.g.*, Wood1 and Wood2) were used to differentiate materials with different dimensions. The wood used in this study is pine wood. Styrofoam is white in color and made of expanded polystyrene foam. The Styrofoam used in this study was obtained from the polystyrene foam racks that were used for holding 50 mL conical bottom centrifuge tubes. The types of metals used has been provided in our previous publication [12].

All experiments were conducted on a benchtop made of stainless steel. Therefore, stainless steel was considered the control background in our experiments. All experiments were conducted in a dark room with room temperature maintained at 21 ± 1 °C without control of the relative humidity in the room. The room's relative humidity and temperature was measured by a humidity monitor (4300 Construction Weather Tracker, Kestrel). Warm water was produced by heating DI water on a hotplate (Isotemp®, Fisher Scientific). Error bars in the figures are standard deviations calculated from repeated experiments of at least 3 times. The infrared images were obtained using an infrared sensing camera (ThermoVision SC-6000, FLIR) located approximately 40 cm directly above the materials and water surface. The ThermoVision SC-6000 camera has a spectral sensitivity range between 3 and 5 μm in wavelength (3333–2000 cm^{-1}) and a temperature sensitivity of 50 mK [13].

2.1. Warm water experiments

We conducted a series of experiments with 30 °C water in Petri-dish containers, which were placed on top of various materials. After pouring 3 mL of 30 °C water into the Petri-dish container and covering it with the lid, the WCC was immediately formed on the inner lid surface due to the temperature difference between the water vapor and the lid [14]. The diameters of the WCCs were tracked afterwards. Materials with different thermal conductivity (**Table S1** in **Supplementary Material**) were tested, including aluminum (Al), Teflon (PTFE), wood, and Styrofoam. As the control, the Petri dish was placed on the edges of two Petri-dish lids, which created a 0.6 cm gap between the bottom of the Petri-dish container and the benchtop (see **Fig. S1a** for details in **Supplementary Material**). A series of control experiments were carried out to check the validity of the control (**Fig. S1b**).

In initial experiments, a Day-Light Lamp, which simulates sunlight with 99.3% UV blocked, was used to explore the influence of light. The presence of light enhanced the reduction of the WCC (**Fig. S2**), probably because light provides energy for the water droplets to evaporate. Therefore, all subsequent experiments were conducted in a dark room without the presence of significant visible light.

2.2. Room-temperature water experiments

Covered Petri-dish containers prefilled with room-temperature water were not able to generate WCCs. Therefore, the first step employed 30 °C water. Once the WCCs formed, the next step was to transfer the lids with the formed WCCs to containers prefilled with room-temperature water. Details are as follows: Petri-dish containers (35 × 10 mm) were placed on Styrofoam. Then 3 mL of 30 °C water was poured into these containers, after which they were covered with lids for 10 min. to create WCCs. With the formed WCCs, the lids were transferred to cover other Petri-dish containers that were pre-filled with 3 mL of room-temperature water, which were placed on different supporting materials. Experiments with larger size Petri dishes (95 × 15 mm) were also conducted. Procedures were similar to those above, except using 15 mL of water instead of 3 mL of water. Experiments were also conducted to check the validity of the control. Control experiments on different materials did not show any significant

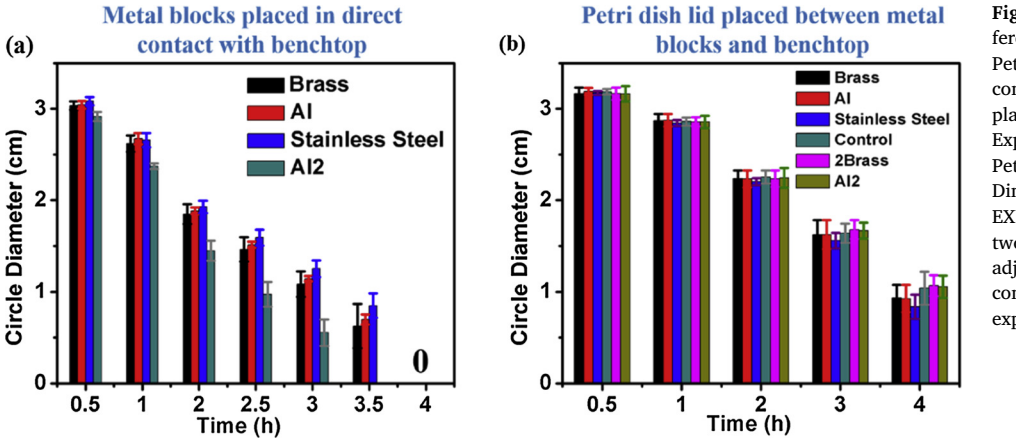

Fig. 4. Diminution of circle diameter with different metals placed beneath the bottoms of Petri dishes. (a) Metal blocks placed in direct contact with benchtop. (b) Petri-dish lids placed between metal blocks and benchtop. Experimental condition: 3 mL of 30 °C water in Petri-dish containers (35 × 10 mm). Dimensions of the materials are listed in the EXPERIMENTAL SECTION, 2Brass indicates two brass metal blocks (1.0 × 1.0 × 0.8 cm) adjoining one another and placed beneath the container bottom. **Figure S8** shows how the experiments were conducted.

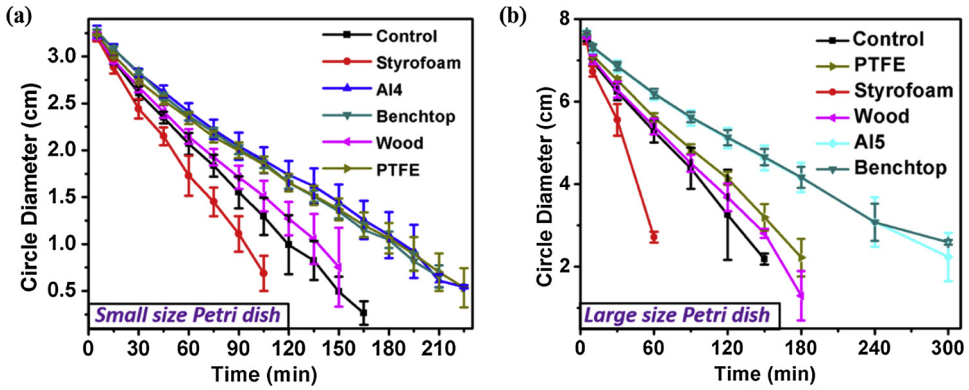

Fig. 5. Diminution of circle diameter with different size Petri dishes. Experimental conditions: (a) 3 mL of room-temperature water in Petri-dish containers (35 × 10 mm); and (b) 15 mL of room-temperature water in Petri-dish containers (95 × 15 mm).

impact on WCC diminution rate (**Fig. S3**).

3. Results and discussion

The WCC decreased following a particular pattern: it diminished stepwise from its edge to the center, one ring at a time, until it completely vanished (Fig. 1). The water droplets in the WCC disappeared through evaporation, turning into water vapor. This happened in all experiments. Although the center of the circle eventually disappeared, the diminution always began at the circle's outer edge, while other parts of the circle remained unchanged. It was a kind of digital phenomenon. This stepwise feature of the diminution pattern could be related to the air circulation in the Petri dish because the dish was not perfectly sealed and water vapor could escape through gaps between the lid and container's edge. The continued mass loss of the system during the experiment (**Fig. S4**) confirmed that the system was losing water, probably because of the water vapor escaped through the aforementioned gaps. When the Petri dish was largely sealed (though incompletely) with plastic wrap or Parafilm, the diminution rate of the WCC was significantly mitigated (**Fig. S5 and S6**). With small holes drilled on the Petri-dish lid and the gaps well-sealed, the water condensation areas progressively diminished starting from the holes (**Fig. S7**), further indicating that air circulation in the Petri dish could impact the water condensation diminution. The stepwise nature of WCC diminution is beyond the scope of this study and requires further investigation.

3.1. Warm water experiments

Notwithstanding their presence *outside* the container, all materials impacted the WCC diminution rate (Fig. 2a). Compared to control, Styrofoam notably prolonged the WCC, while the diminution rates for PTFE and wood were very close to that of the control. Aluminum (Al4 in Fig. 2a), on the contrary, significantly accelerated the diminution. Also, the diminution rate increased further with the increase of aluminum-sample size (Fig. 2b).

The reason for the different WCC diminution rates for the different materials placed outside the Petri dish is an interesting question. The above observations imply that the presence of these supporting materials (Fig. 2a), and their dimensions (Fig. 2b), impact the evaporation rate of the WCC's water droplets. The likely factors that could have an effect are temperature and humidity [14,15]. Fundamentally, evaporation is an endothermic process. We would expect that higher water temperature could result in faster evaporation and thus faster WCC diminution.

We thus measured the temperature of the lid center and the container edge as shown in Fig. 3. To reach plateau temperatures (approximately 21.8 °C), it took 30 min. for Al4, 45 min. for control, and 70 min for Styrofoam. The temperature fluctuations observed during the plateau were probably due to temperature fluctuations in the room. For Styrofoam, the relatively higher temperatures of the lid center before reaching the plateau would be expected to result in the fastest evaporation of its WCC, which is contradictory to what we observed (Fig. 2a). Hence, the temperature of lid center was not the determining factor in WCC evaporation.

We then speculated that it might be the humidity in the Petri dish that played the dominant role in the WCC diminution. Because of technical limitations, we were unable to directly measure the humidity in the Petri dish. As shown in **Fig. S7**, a minor change to the lid could significantly change the water condensation pattern on the lid. Placing wiring into the Petri dish to measure humidity may thus cause undesirable impacts, such as creating water vapor leakages through holes

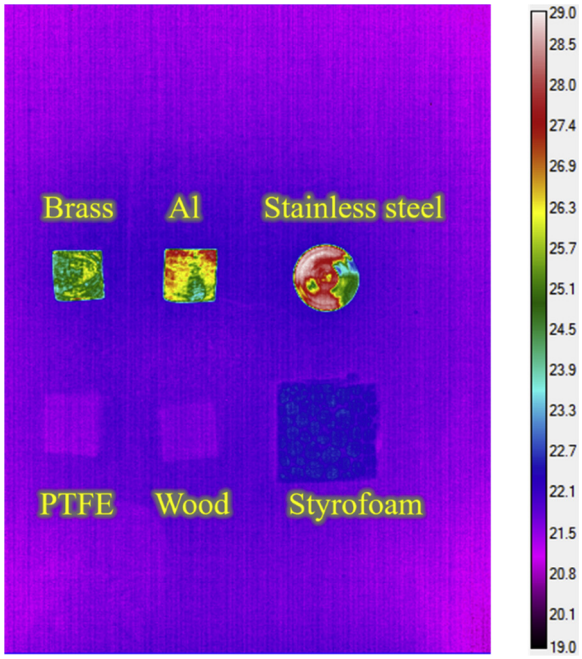

Fig. 6. Infrared images of different materials (*i.e.*, Styrofoam, wood, PTFE, aluminum [Al], stainless steel, brass). The metals showed mosaic-like yellowish and reddish color, indicating their high radiant emission. Those non-metals (*i.e.*, wood and PTFE) were light blue and Styrofoam was dark blue, indicating their low radiant emissions. Color denotes temperature and scale is provided at the right. The IR images (3–5 μm emission band) were taken at room temperature (For interpretation of the references to colour in this figure legend, the reader is referred to the web version of this article).

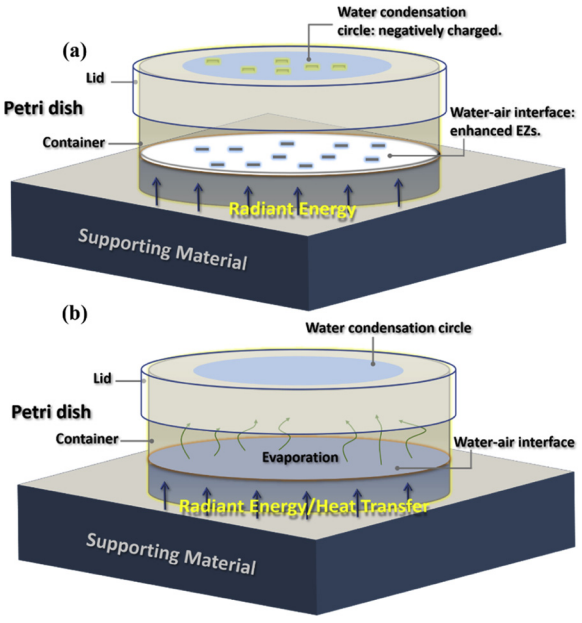

Fig. 7. Diagrammatic sketch of proposed mechanisms for supporting materials impacting WCC diminution. (a) Radiant energy emitted from the supporting material builds negatively charged EZs at the water-air interface. The dashes "-" in the figure indicate negative charges. (b) Radiant energy emitted from the supporting material enhances the kinetic energy of the water molecules at the water-air interface. Alternatively, heat transfer between the supporting material and water in the Petri-dish container impacts water evaporation.

or gaps. Ultrafine humidity measuring technique may be required for future research. The relatively higher temperature of the container edge for the Styrofoam experiment indicated higher water temperature in the container; therefore, it was reasonable to expect faster water evaporation, resulting in more water molecules in the vapor phase in the Petri dish. The Petri dish systems for control, Al4, and Styrofoam showed similar rates of mass loss, from water molecules escaping through the gaps (**Fig. S4**), implying similar rates of water molecules leaving those systems. In other words, the Styrofoam system had more water evaporation, but a similar rate of water escaping the system relative to control- and Al4- systems, which indicated that Styrofoam system retained more water in the vapor phase and thus higher humidity in the Petri dish.

Based on the argument above, that chamber humidity played the dominant role in WCC diminution, it would appear that different supporting materials impact the water temperature in the container, and then its evaporation rate, which in turn results in different humidity in the Petri dish and the different WCC diminution rate. A question arises from this train of logic: how can different supporting materials impact the water temperature in the Petri dish?

This may not be a difficult question to answer. Since the experiments began with a 30 °C water temperature, while other components of the system were at room temperature (21 ± 1 °C), heat transfer from the water to the supporting materials should be significant. As a good thermal insulator, Styrofoam would significantly diminish heat transfer, and hence temperature reduction, of the Petri-dish water. On the contrary, aluminum is a good thermal conductor and facilitates heat transfer; this results in faster temperature reduction of the Petri-dish water, as observed (Fig. 3). With the increase of the size of aluminum, the WCC diminution rate gradually increased (Fig. 2b) and the diminution rate for all these aluminum masses were higher than the control. Since larger aluminum accelerates heat transfer, this result further demonstrated that faster heat transfer and temperature reduction of the container's water could lead to faster WCC diminution rate.

In order to confirm that heat transfer impacts the WCC diminution rate, we conducted another series of experiments with different metals (*i.e.*, brass, stainless steel, and aluminum). The metals were in direct contact with the benchtop (**Fig. S8a**), or placed on Petri-dish lids (**Fig. S8b**). The Petri dish lids were made of polystyrene, which is a good thermal insulator, while these metals are good thermal conductors. When the metals are in direct contact with the benchtop, the heat transfer from the container to the benchtop should be fast. As it turned out, experiments with these metals in direct contact with the benchtop all showed fast WCC diminution (Fig. 4a). However, with Petri dish lids placed between metals and benchtop, an arrangement that should significantly slow down the heat transfer from the container to the benchtop, the WCC diminution rates were notably reduced and similar for all these metals (Fig. 4b). Thus, it was confirmed that heat transfer from the water to the supporting materials and further to the benchtop could impact the WCC diminution rate.

This part of experiments employed 30 °C water, a tepid temperature. We confirmed the impact of heat transfer on WCC diminution. Since the isothermal heat capacity of water has a minimum around 37 °C, water temperature above this particular point may also have interesting effects on WCC diminution. This is beyond the scope of this study, but worthy of further study.

3.2. Room-temperature water

The original goal of this study was to observe the impact of radiant energy generated from different materials on water evaporation and condensation. Therefore, room-temperature water was used for the following experiments to avoid significant heat transfer from water in the container to the supporting materials. Contrary to what we observed with 30 °C water, here we found the opposite: Styrofoam noticeably facilitated the diminution of the WCC, while metals (*i.e.*, aluminum, benchtop [stainless steel]) and PTFE notably prolonged WCC (Fig. 5a). Wood showed modest slowdown. Results were similar with large size Petri dishes (95 × 15 mm), except that PTFE showed notably

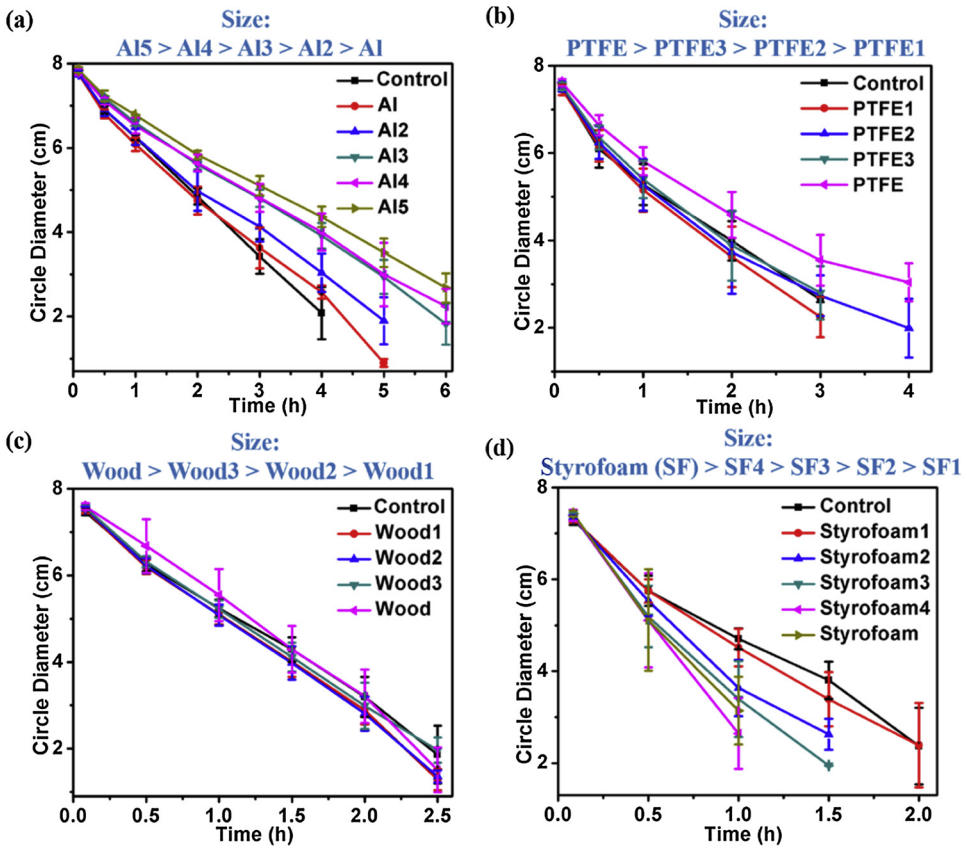

Fig. 8. Effect of material dimensions on the rate of diminution of circle diameter, with the materials placed beneath the Petri dish containers. (a) aluminum; (b) PTFE; (c) Wood; (d) Styrofoam. Experimental condition: 15 mL of room-temperature water in Petri-dish containers (95 × 15 mm).

faster diminution rate than the metals but slightly slower than wood and control (Fig. 5b). This distinct observation for different supporting materials was interesting because no obvious mechanism seems available to explain it.

In this series of experiments carried out with room-temperature water, all experimental apparatus began at room temperature except the lids, which were transferred from covering Petri dish containers prefilled with 30 °C water. All lids, therefore, had WCCs. We recorded the temperature of the lid centers, which decreased to room temperature in less than 1 min. after transferring (data not shown). The amount of heat released by the lids should be negligible because of the small amount of water on the lid, and presumably unable to make a difference in our results.

Radiant energy impacts water evaporation. The most obvious feature of the different supporting materials that could play a role in water evaporation is the differing amounts of radiant energy emitted by those materials. Could radiant energy emitted by the materials have a such compelling impact on the WCC diminution rate? Of the materials studied, those with high radiant emission (*i.e.*, metals) appeared to prolong the WCCs, while materials with low radiant emission (*i.e.*, wood and PTFE) had negligible impact, or even facilitated their diminution (*i.e.*, Styrofoam) [12]. IR has three main subranges: far (FIR, 30– ~200 μm), mid (MIR, 5–30 μm) and near (NIR, 0.7–5 μm). Infrared image (3–5 μm) in NIR range of these materials (Fig. 6) confirms that metals have significantly higher IR emissions than either wood, PTFE, or Styrofoam [12,16]. In our previous study, a similar result of these common materials in terms of IR emission intensity was also observed in the MIR range (7–14 μm) [12].

The high radiant energies emitted by metals (aluminum, brass, and stainless steel) are able to penetrate the Petri-dish container (**Fig. S9a–e**). However, the Petri-dish container completely blocks the radiant energy emitted by PTFE (**Fig. S9a**), while the radiant emission by wood and Styrofoam can be seen indistinctly through the Petri-dish container (**Fig. S9c and e**). With 3 mL of room-temperature water in the Petri-dish containers, the water in the containers with metals placed beneath seemed to be warmer in the infrared images, while PTFE, wood, and Styrofoam did not show any noticeable effect on the water in the containers (**Fig. S9b, d, and f**) [17]. Additionally, as a control, when an IR LED light was placed beneath the Petri dish as a source of radiant energy, the WCC remained constant during the experiment, showing no signs of diminution (**Fig. S10**). These results suggest that radiant energies emitted by the supporting materials may bear the responsibility for modulating the WCC diminution rate.

The above observations suggest that radiant energy could notably impact WCC diminution rate. This raises a question: What is the mechanism by which radiant energy affects the WCC diminution rate? One interpretation follows from previous work on exclusion zones (EZs) at the water-air interface [11]. EZs are interfacial water layers on the micro-scale, and generally bear negative charge [16]. Radiant energy, most notably IR, builds EZs [9,18]. Water droplets are thought to have EZ shells at their surface, which are also negatively charged [16]. Though EZ shells are currently unresolvable by optical microscopy, the water-air interface and water droplet surface have been demonstrated to be negatively charged [19–22]. External materials with higher radiant energy should enhance the EZs at the water-air interface. EZ enhancement could result in increasing repulsion between the negatively charged EZs at the water-air interface and the negatively charged water droplets of the WCC (Fig. 7a). The increasing repulsion might induce deformation of the water droplets of the WCC, which can alter evaporation dynamics of droplets and thus prolong the WCC's existence [23].

Another two possible explanations for the different WCC diminution rates are related to water evaporation (Fig. 7b) [24]. The first explanation employs radiant energy. Water evaporation is thought to

depend significantly on the librational motions of water molecules (*i.e.*, water rotations). Supporting materials with high radiant energy emission (*i.e.*, aluminum) thus enhances evaporation by increasing the kinetic energy of the water molecules at the water-air interface [25]. The water molecules may then turn into water vapor molecules, increasing the humidity inside the Petri dish [15,25,26]. The other explanation is associated with heat transfer. The water in the Petri-dish container evaporates, which requires energy from the ambient (gas phase) as well as the supporting materials by heat conduction [24]. The heat transfer between the supporting material and the water in the container is thus of importance. Supporting materials with good thermal conductivity (*e.g.*, metals) are expected to enhance water evaporation in the Petri dish by expediting heat transfer to the evaporating water [24]. This water evaporation can affect the humidity inside the Petri dish (**Fig. S5–S7**). As demonstrated in previous discussion involving 30 °C water, higher humidity in the Petri dish significantly prolonged the WCC's existence.

If radiant energy modulates the WCC diminution rate, increasing external material size should increase radiant energy and thus prolong the WCC's existence. Materials of different size were tested to explore their impacts on WCC diminution rate. As expected, with the increase of aluminum sizes, the diminution rate of WCCs gradually decreased (Fig. 8a). For PTFE and wood, however, the diminution rates did not show statistically significant differences with size increase, except for the largest size of PTFE (Fig. 8**b** and **c**). Even more interesting was that Styrofoam seemed to display a contrary trend: the diminution rate progressively increased with an increase of Styrofoam size (Fig. 8d).

Careful inspection of the infrared images of the materials (Fig. 6) further suggests that it may not be the quantity of the radiated energy itself but possibly its wavelength range that matters. This is to be expected because emitted radiation must resonate with O—H vibrations of water bonds in order to provide kinetic energy [27,28]. Such inference can be drawn from the observation that Styrofoam, the only material that increased WCC diminution rate, in fact radiates more energy than wood or PTFE (Fig. 6). IR radiation can induce librational motions of water molecules (*i.e.*, water rotations) at wavelengths centered around 4.65 μm and 15 μm [29–31]. Styrofoam probably does not emit in a range effective for inducing water-bond vibration, but rather acts by blocking resonant radiation coming from the environment. This blocking effect increases also with increasing size of the Styrofoam support. Cellulose-based materials (*e.g.*, wood) emit IR mostly at long wavelengths above 7–20 μm [32]. Metallic surfaces, on the other hand, apart from emitting radiant energy, are also effective in reflecting radiation coming from the environment. Aluminum reflects most IR radiation from its surroundings [33,34]. It is also worth noting that IR radiation has been shown to enhance water evaporation more effectively than conductive heating because of its resonance with specific vibrations of water molecules [35,36]. However, all the three explanations provided in this study (*i.e.*, EZ enhancement, water evaporation resulting from enhanced radiant energy and heat transfer) may contribute to the WCC diminution.

In summary, an unexpected phenomenon was identified: the progressive diminution of the water condensation circle (WCC) formed on the inner surfaces of Petri dish lids. Objects placed beneath the bottom of the Petri dishes notably affected the diminution of the WCCs. For systems that were not in thermal equilibrium with the environment (*i.e.*, warm water in the Petri-dish containers), heat transfer played a dominant role in WCC diminution by impacting the humidity in the Petri dish. For systems that were in thermal equilibrium with the environment (*i.e.*, room-temperature water in the Petri dish), radiant energy emitted from different materials, especially metals, appeared to retard the WCC diminution rate by enhancing EZ expansion at the water-air interface or through evaporation of the water in the containers. That common materials placed nearby containers of water can have profound impacts on evaporation rates is surprising, and throws new light on still-unresolved mechanisms of evaporation.

Declaration of Competing Interest

The authors declare that they have no known competing financial interests or personal relationships that could have appeared to influence the work reported in this paper.

Acknowledgements

We appreciate the Software AG foundation (SAGST) for the support of this work. We thank Zheng Li, Kevin Shelton, Abha Sharma, Laura Colton, and Amar Neogi for constructive comments on early versions of the manuscript.

Appendix A. Supplementary data

Supplementary material related to this article can be found, in the online version, at doi:https://doi.org/10.1016/j.colsurfa.2019.123992.

References

[1] J.J. Hegseth, N. Rashidnia, A. Chai, Natural convection in droplet evaporation, Phys. Rev. E 54 (1996) 1640–1644.
[2] H.Y. Erbil, Evaporation of pure liquid sessile and spherical suspended drops: a review, Adv. Colloid Interface Sci. 170 (2012) 67–86.
[3] H. Hou, Q. Bi, X. Zhang, Numerical simulation and performance analysis of horizontal-tube falling-film evaporators in seawater desalination, Int. Commun. Heat Mass Transf. 39 (2012) 46–51.
[4] R. Savino, S. Fico, Transient Marangoni convection in hanging evaporating drops, Phys. Fluids 16 (2004) 3738–3754.
[5] Y. Wang, C. Wang, X. Song, M. Huang, S.K. Megarajan, S.F. Shaukat, H. Jiang, Improved light-harvesting and thermal management for efficient solar-driven water evaporation using 3D photothermal cones, J. Mater. Chem. A Mater. Energy Sustain. 6 (2018) 9874–9881.
[6] F.P.J. Valero, W.D. Collins, P. Pilewskie, A. Bucholtz, P.J. Flatau, Direct radiometric observations of the water vapor greenhouse effect over the equatorial pacific ocean, Science 275 (1997) 1773.
[7] S. Solomon, K.H. Rosenlof, R.W. Portmann, J.S. Daniel, S.M. Davis, T.J. Sanford, G.-K. Plattner, Contributions of stratospheric water vapor to decadal changes in the rate of global warming, Science 327 (2010) 1219.
[8] R. Hołyst, M. Litniewski, D. Jakubczyk, K. Kolwas, M. Kolwas, K. Kowalski, S. Migacz, S. Palesa, M. Zientara, Evaporation of freely suspended single droplets: experimental, theoretical and computational simulations, Rep. Prog. Phys. 76 (2013) 034601.
[9] B. Chai, H. Yoo, G.H. Pollack, Effect of radiant energy on near-surface water, J. Phys. Chem. B 113 (2009) 13953–13958.
[10] J.-M. Zheng, W.-C. Chin, E. Khijniak, E. Khijniak Jr., G.H. Pollack, Surfaces and interfacial water: evidence that hydrophilic surfaces have long-range impact, Adv. Colloid Interface Sci. 127 (2006) 19–27.
[11] A.J. Mork, G.H. Pollack, New observations at the air-water interface, J. Undergraduate Res. Bioengineering (2012) 105–113.
[12] K.W. Kimura, G.H. Pollack, Particle displacement in aqueous suspension arising from incident radiant energy, Langmuir 31 (2015) 10370–10376.
[13] I. Rad, G.H. Pollack, Cooling of pure water at room temperature by weak electric currents, J. Phys. Chem. B 122 (2018) 7711–7717.
[14] J.E. Finer, J.J. Finer, A simple method for reducing moisture condensation on Petri dish lids, Plant Cell Tissue Organ Cult. 91 (2007) 299–304.
[15] J. Ferguson, The rate of natural evaporation from shallow ponds, Aust. J. Chem. 5 (1952) 315–330.
[16] G.H. Pollack, The Fourth Phase of Water: Beyond Solid, Liquid, and Vapor, Ebner and Sons Publishers, Seattle, WA, 2013.
[17] R. Viskanta, J.S. Toor, Radiant energy transfer in waters, Water Resour. Res. 8 (1972) 595–608.
[18] Q. Zhao, J. Zheng, B. Chai, G.H. Pollack, Unexpected effect of light on colloidal crystal spacing, Langmuir 24 (2008) 1750–1755.
[19] A.V. Shavlov, V.A. Dzhumandzhi, A.A. Yakovenko, Charge of water droplets during evaporation and condensation, J. Aerosol Sci. 123 (2018) 17–26.
[20] A.V. Shavlov, Electrical processes upon the evaporation and condensation of water and ice, Colloid J. 71 (2009) 263–270.
[21] M. Takahashi, ζ potential of microbubbles in aqueous solutions: electrical properties of the gas – water Interface, J. Phys. Chem. B 109 (2005) 21858–21864.
[22] K. Ciunel, M. Armélin, G.H. Findenegg, R. von Klitzing, Evidence of surface charge at the air/water interface from thin-film studies on polyelectrolyte-coated substrates, Langmuir 21 (2005) 4790–4793.
[23] J.Y. Kim, I.G. Hwang, B.M. Weon, Evaporation of inclined water droplets, Sci. Rep. 7 (2017) 42848.
[24] S. David, K. Sefiane, L. Tadrist, Experimental investigation of the effect of thermal properties of the substrate in the wetting and evaporation of sessile drops, Colloids Surf. A Physicochem. Eng. Asp. 298 (2007) 108–114.
[25] C.C. Tseng, R. Viskanta, Enhancement of water droplet evaporation by radiation absorption, Fire Saf. J. 41 (2006) 236–247.

[26] M.Q. Brewster, Evaporation and condensation of water mist/cloud droplets with thermal radiation, Int. J. Heat Mass Transf. 88 (2015) 695–712.
[27] K. Ramasesha, L. De Marco, A. Mandal, A. Tokmakoff, Water vibrations have strongly mixed intra- and intermolecular character, Nat. Chem. 5 (2013) 935.
[28] J.P. Meng, X.L. Huo, J. Liu, Y.F. Pan, Influence of tourmaline mineral material on structure and physical and chemical properties of water, Appl. Mech. Mater. 320 (2013) 577–583.
[29] B. Mizaikoff, Waveguide-enhanced mid-infrared chem/bio sensors, Chem. Soc. Rev. 42 (2013) 8683–8699.
[30] Y. Tong, T. Kampfrath, R.K. Campen, Experimentally probing the libration of interfacial water: the rotational potential of water is stiffer at the air/water interface than in bulk liquid, Phys. Chem. Chem. Phys. 18 (2016) 18424–18430.
[31] C.D. Cappa, J.D. Smith, W.S. Drisdell, R.J. Saykally, R.C. Cohen, Interpreting the H/D isotope fractionation of liquid water during evaporation without condensation, J. Phys. Chem. C 111 (2007) 7011–7020.
[32] C. Hyll, Infrared Emittance of Paper —method Development, Measurements and Application, in: Industrial Engineering and Management, Royal Institute of Technology (KTH): Stockholm, 2012.
[33] V. Bernard, E. Staffa, V. Mornstein, A. Bourek, Infrared camera assessment of skin surface temperature – effect of emissivity, Phys. Medica 29 (2013) 583–591.
[34] J. Bartl, M. Baranek, Emissivity of aluminum and its importance for radiometric measurement, Meas. Sci. Rev. 4 (2004) 31–36.
[35] M.A. Rösler, E. Klinke, G. Kunz, Evaporation of solvents by infrared radiation treatment, Prog. Org. Coat. 23 (1994) 351–362.
[36] R. Joseph, E.P. Guyer, R. Thelen, Sick of watching paint dry?: decrease drying times with your existing paint booth by tweaking temperature, air velocity, and relative humidity, J. Met. Finish. Soc. Jpn. 105 (2007) 44–50.